Chapter

Kesterite $Cu_2ZnSnS_{4-x}Se_x$ Thin Film Solar Cells

Kaiwen Sun, Fangyang Liu and Xiaojing Hao

Abstract

Kesterite $Cu_2ZnSnS_{4-x}Se_x$ (CZTS) is a promising thin film photovoltaic (PV) material with low cost and nontoxic constitute as well as decent PV properties, being regarded as a PV technology that is truly compatible with terawatt deployment. The kesterite CZTS thin film solar cell has experienced impressive development since its first report in 1996 with power conversion efficiencies (PCEs) of only 0.66% to current highest value of 13.0%, while the understanding of the material, device physics, and loss mechanism is increasingly demanded. This chapter will review the development history of kesterite technology, present the basic material properties, and summarize the loss mechanism and strategies to tackle these problems to date. This chapter will help researchers have brief background knowledge of kesterite CZTS technology and understand the future direction to further propel this new technology forward.

Keywords: kesterite, $Cu_2ZnSn(S,Se)_4$, CZTS, thin film solar cells, loss mechanism

1. Introduction

Thin film photovoltaic (PV) technologies such as $Cu(In,Ga)Se_2$ (CIGS) and CdTe have already demonstrated more than 20% power conversion efficiency (PEC) [1, 2] and are at their commercial stage. However, considering the Restriction of Hazardous Substances Directive (RoHS) adopted in European Union [3] and the recent classification of critical raw materials (CRM) by the European Commission [4], emerging thin film PV technologies with RoHS-compliant and CRM-free constituents are increasingly desirable. Kesterite copper-zinc-tin-selenosulfide and related quaternary semiconductor represented by chemical formula $Cu_2ZnSnS_{4-x}Se_x$ is generally accepted as one promising option for low-cost and nontoxic thin film PV.

The family of kesterite $Cu_2ZnSnS_{4-x}Se_x$ includes pure sulfide Cu_2ZnSnS_4 (CZTS), pure selenide $Cu_2ZnSnSe_4$ (CZTSe), and selenosulfide $Cu_2ZnSn(S,Se)_4$ (CZTSSe) and other related compound semiconductors. Herein we abbreviate all $Cu_2ZnSnS_{4-x}Se_x$ compounds as CZTS. The formation of CZTS is derived from cation mutations (cross-substitutions) in $CuInS_2$ by replacing two In atoms with one Zn and one Sn [5, 6]. CZTS possess high absorption coefficient of over 10^4 cm^{-1}, tunable band gap that can range from 1.0 to 1.5 eV to favorably match the solar spectrum, intrinsic p-type conductivity, and a three-dimensional symmetry of carrier transport [7–9]. These decent photovoltaic properties of CZTS have attracted considerable attention and enabled its rapid development in the last decades. The highest power conversion efficiencies (PCEs) of Cu_2ZnSnS_4, $Cu_2ZnSnSe_4$

and $Cu_2ZnSn(S,Se)_4$ have been set to 11%, 12.5%, and 13%, respectively [10–12], which represent the best PCE among the emerging RoHS-compliant and CRM-free inorganic thin-film PV technologies.

In this chapter, the development history and current status of CZTS PV technology will be briefly introduced. The basic physical and chemical properties of CZTS thin film will be described to help readers have a better understanding of the material. The device architecture and absorber processing will be touched; finally. The limiting factors as well as the perspective for future development of this technology will also be reviewed and addressed.

2. The development history of CZTS

The CZTS single crystal was first grown by Nitsche, Sargent, and Wild in 1966 when they tried to prepare a serious of $A^I_2B^{II}C^{IV}X_4$-type quaternary chalcogenides using iodine vapor transport [13]. The photovoltaic effect of CZTS was exhibited for the first time in 1988 by Ito and Nakazawa on a heterojunction diode consisting of cadmium-tin-oxide transparent conductive layer and CZTS thin film on a stainless steel substrate. The open-circuit voltage was measured to be 165 mV under AM1.5 illumination [14]. The open-circuit voltage was increased to 250 mV after annealing the device in air, and short-circuit current of 0.1 mA/cm^2 was achieved [15].

The first CZTS solar cell with PCE of 0.66% was reported by Katagiri et al. in 1996 at PVSEC-9, with the device structure of ZnO:Al/CdS/CZTS/Mo/soda lime glass (SLG) substrate [16]. The CZTS thin film was fabricated by vapor-phase sulfurization of E–B-evaporated precursors [17]. In 1997, Friedlmeier et al. reported the CZTS solar cell with PCE of 2.3% and open-circuit voltage of 570 mV based on thermal evaporation [18]. In 1999, the Katagiri group improved the PCE up to 2.63% [19], after that they did a lot of work on optimizing the CZTS thin film and pushed the efficiency to 5.74% until 2007 [19–24].

The CZTS solar cell started to gain intensive interest from academic and industry community from 2008 when its efficiency was further boosted to 6.7% by Katagiri et al. and when the CIGS solar cell became mature in its commercialization stage [25]. A lot of research institutes and solar cell manufactures such as Toyota, IBM, NREL (National Renewable Energy Laboratory), Solar Frontier, EMPA (Swiss Federal Laboratories for Materials Science and Technology), HZB (Helmholtz-Zentrum Berlin), ZSW (Centre for Solar Energy and Hydrogen Research Baden-Württemberg), UNSW (University of New South Wales), and so on involved in the development of this technology and significant advances have been achieved in the following decade [10, 26–33]. During the development period, Se incorporation has attracted significant attention and led to impressive progress in PCE [34–37]. Moreover, various fabrication methods including vacuum deposition process and non-vacuum process such as solution method, electrochemical deposition, etc., have been developed for fabricating the CZTS thin film [29, 37–40].

An important milestone in the development of CZTS solar cell is the 10% benchmark efficiency breakthrough achieved by IBM Thomas J. Watson Research Center in 2011 [34], which shows substantial commercial promise for the CZTS-based class of thin film PV materials. This breakthrough also established the leading position of IBM in CZTS PV technology research, represented by a serious of world record efficiencies [38, 39, 41]. The highest PCE for CZTS solar cell has been stagnant at 12.6% for more than 6 years since 2014 when IBM last updated their efficiency breakthrough [39]. Thanks to the better understanding of the CZTS material and the loss mechanism of the device, quite a few groups reported CZTS PCE close to

the 12.6% record efficiency in recent years [11, 42–46]. The recently announced NREL Best Research-Cell Efficiency Chart included the newly refreshed CZTS record efficiency of 13% achieved by Xin et al. from NJUPT [12]. This small step breakthrough comes from great efforts in this research area and hopefully will bring more interests and confidence to the CZTS R&D community.

3. The physical and chemical properties of CZTS thin film

The investigation and understanding of nature of the CZTS thin film are crucial for further developing this technology. Intensive studies have been conducted during the rapid development stage; therefore, the physical and chemical properties of CZTS have been well revealed.

3.1 Crystal structure

As we briefly introduced earlier, CZTS is derived from the cation mutations of $CuInS_2$ (CIS), while both are originated from the binary II–VI semiconductors adopting the cubic zinc-blende (or hexagonal wurtzite) structure as shown in **Figure 1**.

Similarly, the structure of CZTS is also derived from ternary I-III-VI_2 compounds. In general, as shown in **Figure 2**, chalcopyrite (CH) and CuAu-like (CA) structures are two fundamental I-III-VI2 structures that obey the octet rule [5, 47, 48]. Therefore, the quaternary CZTS is well known as two principal structures, kesterite (space group ***I*4**, **Figure 2d**) and stannite-type (space group ***I*42m**, **Figure 2e**), which are derived from CH structure and CA structure, respectively. Other primitive mixed CA structure (PMCA) (space group ***I*42m**, **Figure 2f**) derived from CA structure has also been reported in CZTS [5, 47, 48]. As the most common structures discussed in literature are kesterite and stannite-type, we only focus on these two structures in this section. The two structures are closely related with the main difference of cation arrangement. Both structures are composed of a cubic close-packed lattice of S anions, with half of the tetrahedral interstices occupied by cations. Sn atoms occupy the same fixed positions in both structures, but the Cu and Zn atoms are in different position [49, 50]. In kesterite structure, cation layers of CuZn, CuSn, CuZn, CuZSn alternated at z = 0, ¼, ½, and ¾ respectively (**Figure 2d**), while in stannite structure, ZnSn and Cu_2 layers alternate with each other (**Figure 2e**). The similarities of structure make it difficult to distinguish kesterite and stannite experimentally by employing common X-ray diffraction and

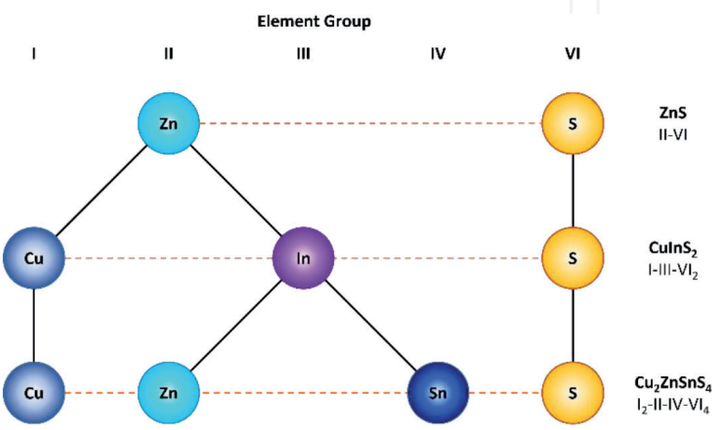

Figure 1.
Schematic illustration of the origin of CZTS structure. Reproduced from [6] with permission from the Royal Society of Chemistry.

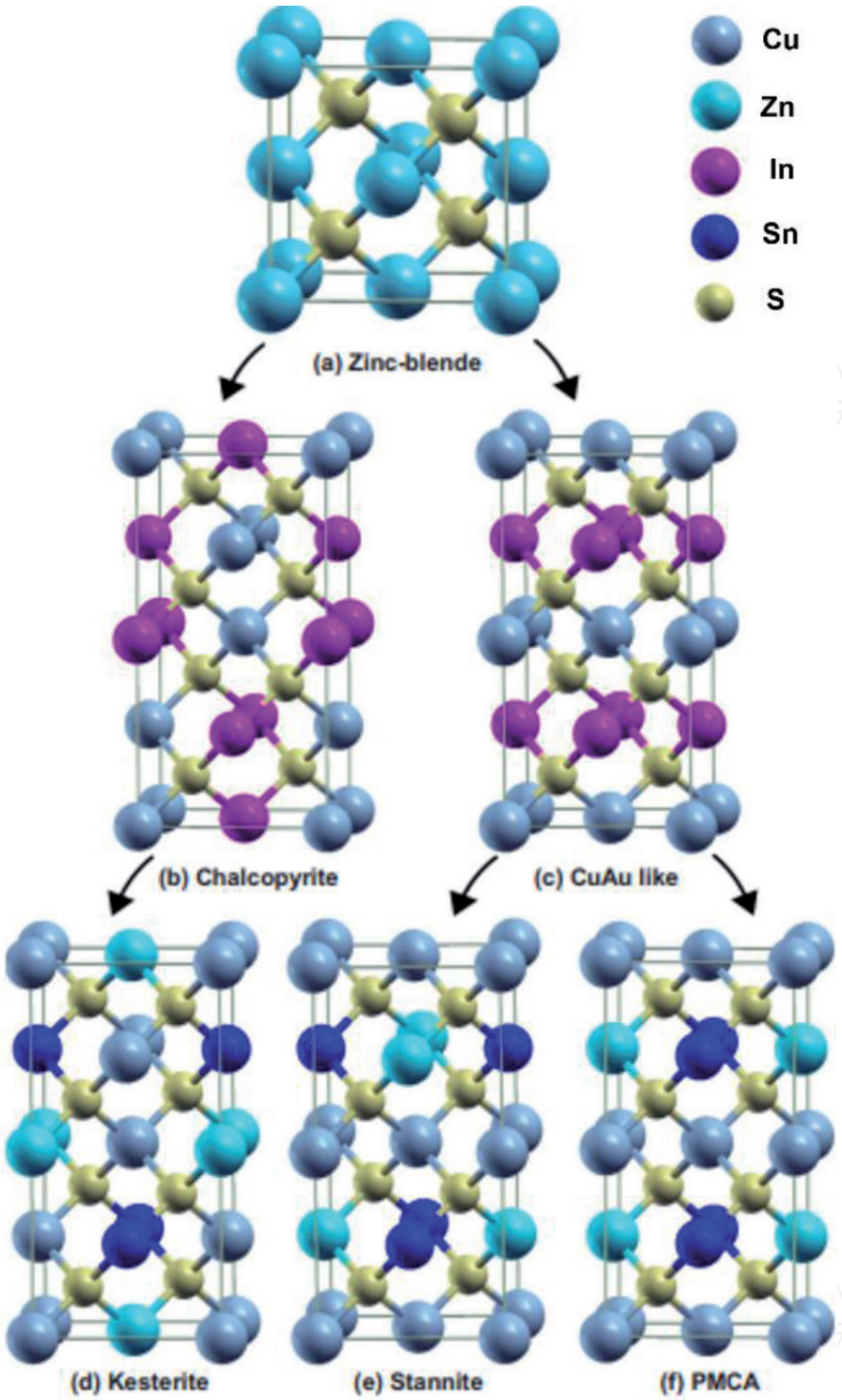

Figure 2.
The crystal structure of (a) zinc-blende ZnS, (b) chalcopyrite $CuInS_2$, (c) CuAu-like $CuInS_2$, (d) Kesterite-type Cu_2ZnSnS_4, (e) stannite-type Cu_2ZnSnS_4, and (f) PMCA-Cu_2ZnSnS_4. Reproduced from [47] with permission from the American Physical Society.

Raman spectroscopy techniques [51, 52]. Only advanced techniques such as neutron powder diffraction analysis are capable to tell them apart [50, 53].

CZTS usually exists as kesterite-type structure, which is more stable thermodynamically than the stannite-type [54]. This is in agreement with the experimental observation [21, 50, 55, 56]. Plenty of theoretical studies have also confirmed that the kesterite-type structure is the ground state structure in CZTS [5, 47, 48, 57–59]. This is also the reason that CZTS is named after Kesterite because it crystallizes as kesterite structure. However, the energy difference between the kesterite and the

stannite-type structure is rather small [5, 47, 48, 57–59]. This indicates that kesterite structure should be formed under equilibrium growth conditions, but both phases may exist, especially when growth method and conditions are changed, it should be relatively easy to grow materials with mixed phases. This may also partly explain the existence of disorder structure with more random distribution of the Cu and Zn on the cation positions [60], which will be discussed in more details in the following sections.

3.2 Electronic band structure

Kesterite CZTS has a similar tetrahedral bonds geometry as traditional group I–V, III–V, and II–VI semiconductors. It obeys Lewis' octet rule with eight electrons around each anion atom (S or Se); the four bonds of each anion therefore form together a close valence shell [48]. However, there are fundamental differences between the Cu-based quaternary compound and the group I–V, III–V, and II–VI binary semiconductors. First of all, the bonds in CZTS involve Cu-d–anion-p hybridized antibonding states. This weakens the bonds in CZTS. Second, Cu in CZTS has only one valence s-like electron while the group III–V (group II–VI) semiconductors have three (two) valence s-like electrons for their cations.

Several first principle studies have revealed the electronic band structure of CZTS [47, 48, 58, 59, 61, 62]. An example is as shown in **Figure 3**, the calculated band structures of kesterite Cu_2ZnSnS_4 and $Cu_2ZnSnSe_4$ from different methods are presented. Overall, the kesterite CZTS materials are all direct-gap semiconductors. Different calculation methods generated slightly different values, for example, generalized gradient approximation (GGA) method calculated the band gap energy for Cu_2ZnSnS_4 and $Cu_2ZnSnSe_4$ as 1.56 eV and 1.05 eV, respectively. Corresponding band gap values from hybrid functional calculations (HSE06) are 1.47 and 0.90 eV, while the values from the GW_0 calculation are 1.57, and 0.72 eV. These values are in agreement with other calculated data and available experimental measurement, converging to the results that Eg ≈ 1.5 eV in CZTS and Eg ≈ 1.0 eV in CZTSe [14, 24, 28, 64–72] to vary linearly as a function of the Se content x [73] with Eg = 1.47, 1.30, 1.17, 1.01, and 0.90 eV for x = 0, 1/4, 1/2, 3/4, and 1, using the HSE06 potential. This linear relationship also agrees with experimental results [66, 70, 71].

The density of states (DOS) of kesterite Cu_2ZnSnS_4 and $Cu_2ZnSnSe_4$ can also be calculated as illustrated in **Figure 4** [63]. It is not surprising to see that Cu_2ZnSnS_4 and $Cu_2ZnSnSe_4$ show comparable DOS as they are in same tetrahedral bond geometries. The DOS of conduction bands in Cu_2ZnSnS_4 is ~0.5 eV higher than that of $Cu_2ZnSnSe_4$ because of large energy gap. It is common that in Cu-based chalcogenides including the quaternary (for example, CIS) and ternary compounds (for example, CZTS), the valence band maximum (VBM) is derived mainly from the hybridization of anion p and Cu d states because Cu has higher d orbital energy than Zn, Ga, In, and Sn [59, 74]. In CZTS, the valence p level of S is lower in energy than Se, thus the VBM of the sulfides is lower than that of the selenides. This difference is reduced by anion p–Cu d overlap (p-d hybridization) because the hybridization is stronger in the shorter Cu–S bond and pushes the antibonding VBM level of the sulfide up relative to that of the selenide. Therefore, the valence band offset between the Cu_2ZnSnS_4 and $Cu_2ZnSnSe_4$ is less than 0.2 eV. The DOS of the CZTS conduction band minimum (CBM) is primarily controlled by the Sn-s and anion p-like states due to the lower s orbital energy of Sn than the other cations [59, 74]. More importantly, in CZTS the lowest CB is separated from the higher energy bands and is therefore more localized in energy. Therefore, the CBM of CZTS is expected to vary depending on the alloying on the Sn-site with other group-IV elements

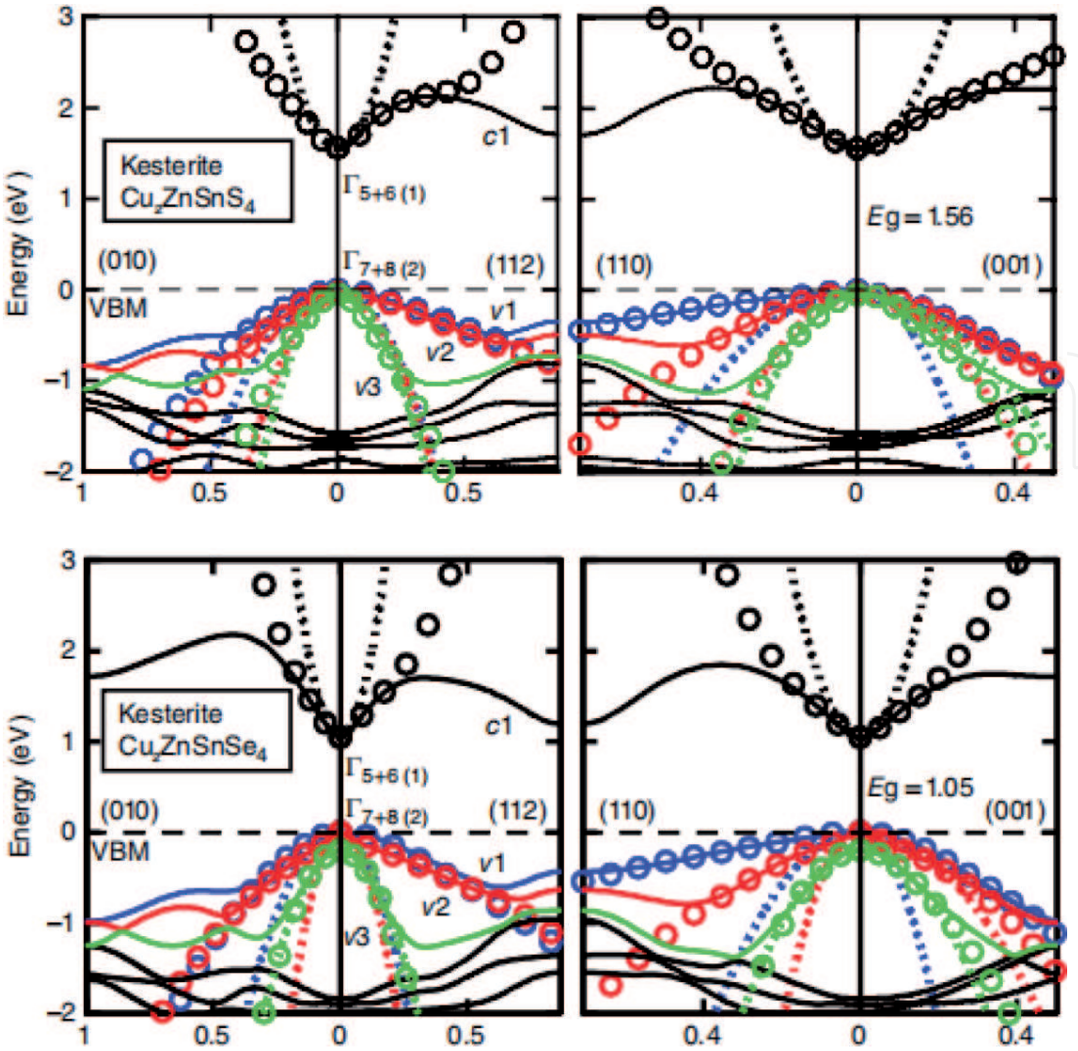

Figure 3.
The electronic band structure of the kesterite structures of Cu_2ZnSnS_4 and $Cu_2ZnSnSe_4$ along four symmetry directions. The energy refers to the VBM (dashed lines). The spin–orbit interaction is included, but the index of the bands refers to spin-independent bands where c1 represents the lowest CB and v1 represents the topmost VB. Different line shapes represent different calculation methods [63]. Reproduced from [59] with permission from American Institute of Physics.

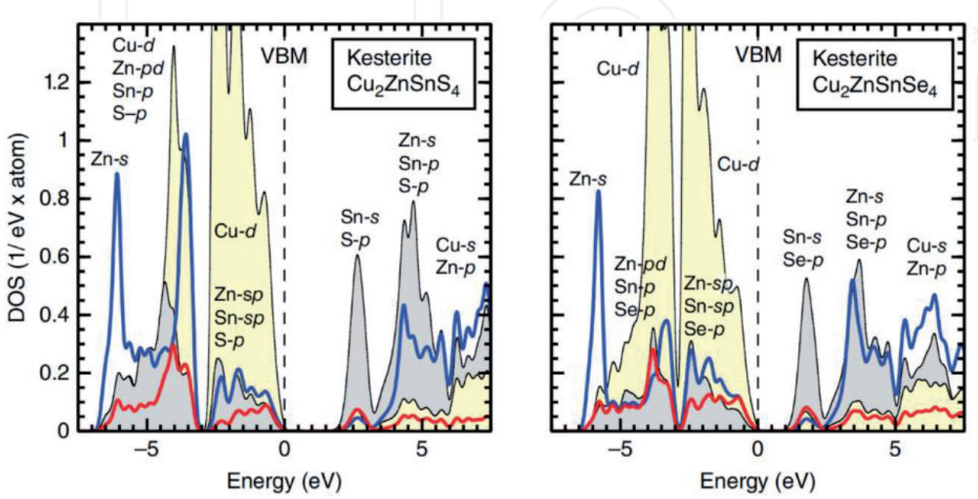

Figure 4.
Atomic and angular momentum resolved DOS of kesterite Cu_2ZnSnS_4 and $Cu_2ZnSnSe_4$ presented with a 70 meV Lorentzian broadening. Reproduced from [59] with permission from American Institute of Physics.

(e.g., Ge) due to this localized CB. The band gap energy can therefore be tailored by cation alloying for an optimized optical efficiency of the materials.

3.3 Composition variation and phase competition

As a quaternary semiconductor, CZTS consists of three metals and up to two chalcogens, which provides a wide range for composition variation and secondary phase formation. However, high-efficiency CZTS thin film solar cells require single-phase kesterite absorber, and some secondary phases have been reported detrimental to the device performance. This section reviews the stable phase region of CZTS and possible secondary phases likely to be formed in the quaternary system.

The 3D CZTS quaternary phase diagram as shown in **Figure 5** can be deduced from Cu_2S-ZnS-SnS_2 pseudo-ternary diagram [77] and CuS-ZnS-SnS pseudo-ternary phase diagram [75] (selenide kesterite system also refers to Cu_2SnSe_3–$SnSe_2$–ZnSe diagram [78]. In addition, the stability region of the CZTS in the atomic chemical potential space can be calculated as shown in **Figure 5** [76, 79]. All these diagrams indicate that volume of the stable CZTS region is small, and the slight deviation (maximum 1–2 at%) outside this space will cause the formation of different secondary phases [5, 80]. The narrow stable window also implies that the composition control and the chemical potential control are crucial for the growth of high-quality and single-phase CZTS absorber. The Zn content is particularly important because the stable region along the μ_{Zn} axis is much narrower. Moreover, it is well accepted experimentally and theoretically that high-efficiency solar cells need CZTS absorber with Zn-rich and Cu-poor composition [8–10, 27, 28, 33, 67, 81]. This makes it more difficult to control the secondary phases formation.

According to the phase diagram and literature report, the most common secondary phases in the Cu-Zn-Sn-S/Se system are list in **Table 1** [92]. The influence of the secondary phases on the solar cell performance depends on their position in the film as well as their physical properties. For example, $Cu_2S(Se)$ phases in the final film may act as shunting path due to both the high conductivity and contact with front and back interfaces. However, $Cu_2S(Se)$ is also an important fluxing agent to promote lateral grain growth during the film growth [28]. Generally, If the secondary phase has a lower band gap than the CZTS absorber, it will limit the open-circuit

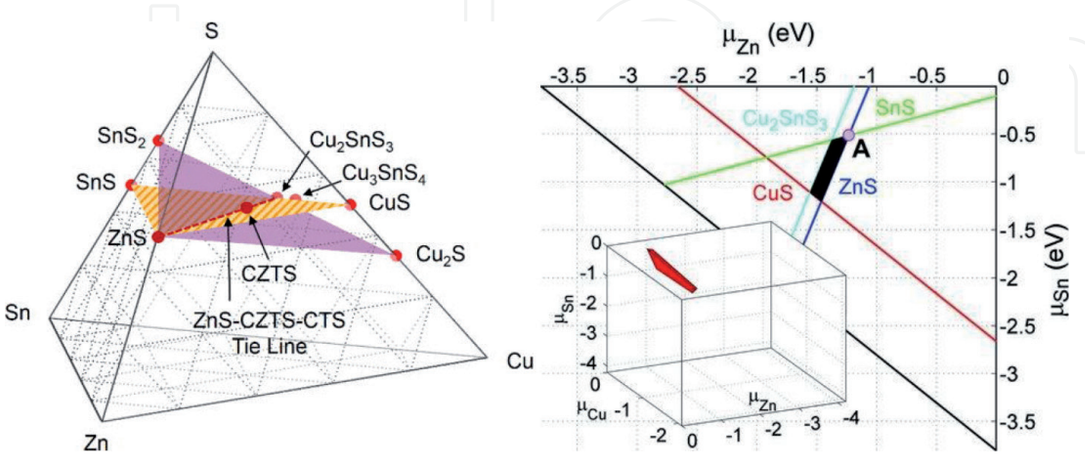

Figure 5.
Left: CZTS quaternary phase diagram including the known phases. Reproduced from [75] with permission from American Institute of Physics. Right: The calculated chemical-potential stability diagram of Cu2ZnSnS4 in a 2D Cu-rich plane (the stable 3D region is inset) reproduced from [76] with permission from American Institute of Physics.

Compound	Band gap (eV)	Ref.	Compound	Band gap (eV)	Ref.
Cu_2ZnSnS_4	1.5	[80]	$Cu_2ZnSnSe_4$	1.0	[80]
Cu_2SnS_3	1.0	[82]	Cu_2SnSe_3	0.8	[83]
ZnS	3.7	[84]	ZnSe	2.7	[84]
SnS_2	~2.5	[85]	$SnSe_2$	1.0–1.6	[86]
SnS	1.0 indirect, 1.3 direct	[87, 88]	SnSe	1.3	[89]
Cu_2S	1.2	[90]	Cu_2Se	1.2	[91]

Table 1.
Most common secondary phases in the Cu-Zn-Sn-S/Se system.

voltage of the solar cell. While secondary phases with higher band gaps than CZTS are less detrimental; however, they can block the transport when present in large amounts [93] or at least increase the series resistance [94]. ZnS(e) is the most likely secondary phase considering the phase diagram and especially when adapting the Zn-rich and Cu-poor condition. Fortunately, ZnS(e) is a large band gap compound and is expected to be rather benign if present in small amounts. It has even been reported that ZnS with similar crystalline structures to CZTS may passivate grain boundaries or heterojunction interface [81, 95, 96] by reducing strain and lowering recombination velocities at the grain interfaces. The tin compounds are unlikely to form because they are usually volatile [97] and will evaporate in most preparation conditions. As shown in **Table 1**, one unfavorable low band gap secondary phase in both Cu_2ZnSnS_4 and $Cu_2ZnSnSe_4$ system is the ternary $Cu_2SnS(e)_3$, which is also one reason for optimal composition range (Zn-rich and Cu-poor) found for the best solar cells. However, the non-homogeneous composition across the CZTS film under normal preparation conditions still provides the possibility to form such detrimental secondary phases [98]. Therefore, how to control the amount and position of the secondary phases in the CZTS absorber needs to be elaborately studied.

3.4 Lattice defects

The formation and properties of lattice defects are important parameters of semiconductor materials and are crucial to the function of photovoltaic devices, because they directly influence the generation, separation, and recombination of electron–hole pairs. The lattice defects (e.g., vacancies, interstitials, antisites) in kesterite CZTS system are complicated because of the increased number of component elements and the similar cation size as well as small chemical mismatch of Cu^+ and Zn^{2+}. In this section, the formation and ionization of the lattice defects in kesterite will be briefly reviewed. More importantly, the underlying mechanism of p-type conductivity, Zn-rich and Cu-poor condition growth condition, as well as limiting factors for device performance in kesterite CZTS solar cells from the perspective of lattice defects will be discussed.

The concentration of the lattice defects is determined by their formation energy. In **Figure 6**, the calculated formation energies of different defects are plotted as functions of the Fermi energy (0 means that the Fermi energy is at VBM, while 1.5 or 1.0 eV means that Fermi energy is at CBM). It is obvious that in both Cu_2ZnSnS_4 and $Cu_2ZnSnSe_4$, Cu_{Zn} antisite is the lowest energy defects, which is different from the defect properties of their parent compounds ($CuInSe_2$ or $CuGaSe_2$) where the dominant defect is the Cu vacancy V_{Cu} [76, 79, 99]. In addition, the formation energies of most acceptor defects are lower than those of donor defects, explaining the intrinsic p-type conductivity observed in literature [21, 48, 64, 84, 100–110].

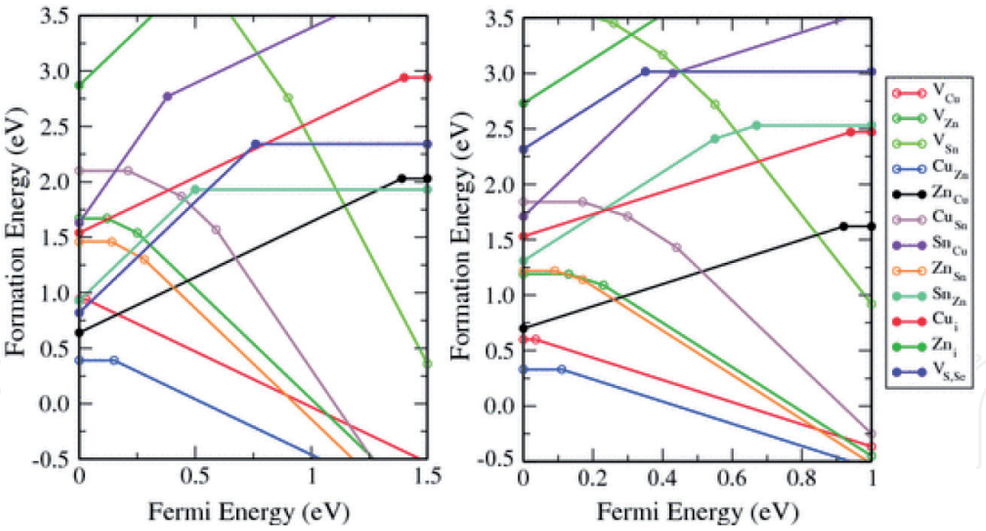

Figure 6.
Calculated defect formation energy as a function of the Fermi energy at the thermodynamic chemical-potential point a (from ***Figure 5*** *right) for Cu_2SnZnS_4 (left) and $Cu_2SnZnSe_4$ (right). For each value of the Fermi energy, only the most stable charge state is plotted, with the filled circles (change of slope) representing a change in charge state (transition energy level). Reproduced from [76, 79] with permission from American Institute of Physics and American Physical Society.*

Another important parameter of lattice defects is their ionization (transition) levels, which determines if they can produce free carriers and contribute to the electrical conductivity. The calculated ionization levels of intrinsic defects in the band gap of Cu_2ZnSnS_4 and $Cu_2ZnSnSe_4$ are shown in **Figure 7**. First of all, in both cases, the dominant defect Cu_{Zn} has an acceptor level (0.11 eV and 0.15 eV above VBM in $Cu_2ZnSnSe_4$ and in Cu_2ZnSnS_4, respectively) deeper than that of V_{Cu}. The relatively deep level of dominant antisite defect in CZTS is not favorable to the device performance because it will limit the open-circuit voltage. This also partially explains why Zn-rich and Cu-poor condition has normally been found to beneficial to solar cell efficiency because it could decrease the formation energy and enhance the population of shallow V_{Cu}. The other acceptor defects (e.g., Cu_{Sn}, Zn_{Sn}, V_{Zn}, and V_{Sn}) have higher formation energy; therefore, they have negligible contribution to the p-type conductivity. However, they may act as recombination centers especially for those deep transition levels such as (4−/3-) and (3−/2-) in band gap as seen in **Figure 7**.

In addition to the point defects, various self-compensated defect clusters can be formed in CZTS due to the large amount of low-energy intrinsic defects. Defect compensation in ternary CIS is well known to have electrically benign character because the intrinsic defects undergo self-passivation through the formation of defect complexes such as $[2V_{Cu}^{-} + In_{Cu}^{2+}]$. Therefore, it is also interesting to see if the same behavior can be observed in quaternary kesterites. Cu_{Zn} and Zn_{Cu} are the lowest-energy acceptor and donor defects, respectively; therefore, antisite pair $[Cu_{Zn}^{-} + Zn_{Cu}^{+}]$ also shows extremely low formation energy. Fortunately, its impact on the electronic structure and optical properties is relatively weak. The detrimental defect clusters are those composed of deep level defects, such as Sn_{Zn}, Sn_{Cu}, Cu_{Sn}, and Zn_i. For example, clusters with Sn_{Zn} induce large conduction band edge downshift, which could limit the solar cell performance, because the induced states are deep and may trap photo-generated electrons from the high conduction band. $[2Cu_{Zn} + Sn_{Zn}]$ clusters could present in high population if in single-phase CZTS (Cu/(Zn + Sn) and Zn/Sn ratios near 1) chemical potential conditions and be detrimental to the solar cell performance. The Zn-rich and Cu-poor condition could prevent the formation of $[2Cu_{Zn} + Sn_{Zn}]$ clusters because its formation energy

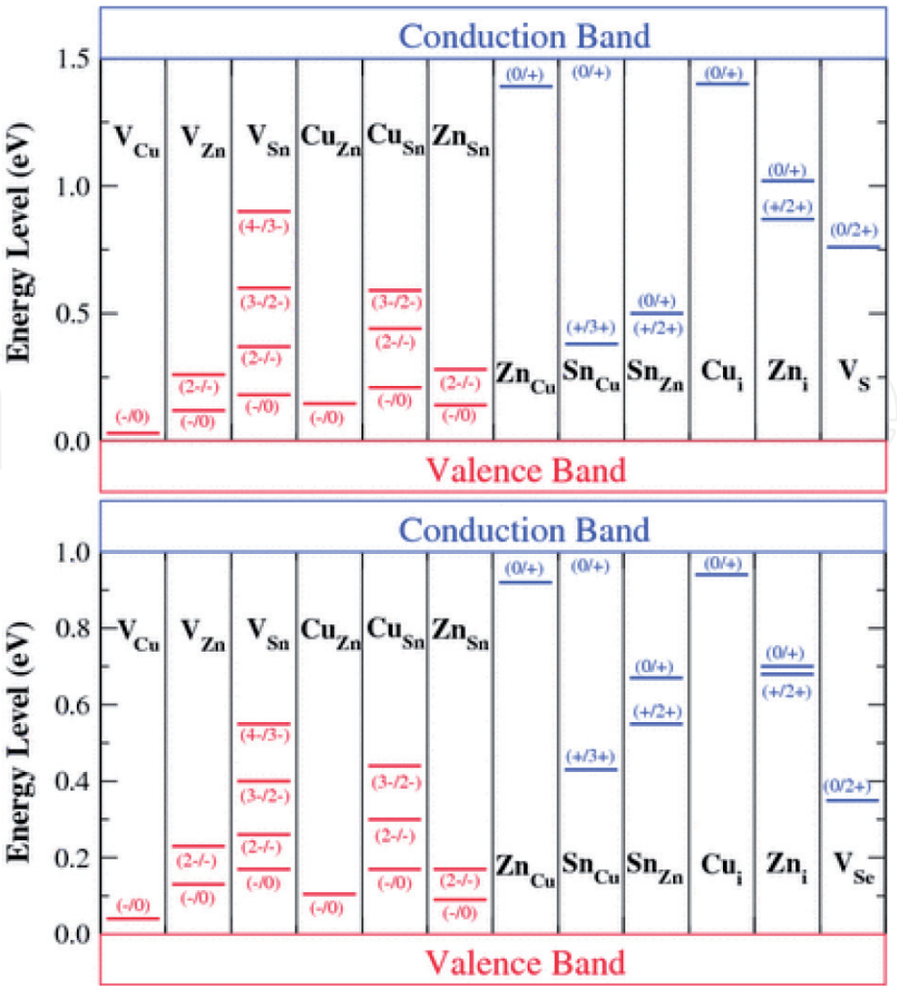

Figure 7.
The ionization levels of intrinsic defects in the band gaps of Cu_2ZnSnS_4 (top) and $Cu_2ZnSnSe_4$ (bottom). The red bars show the acceptor levels, and the blue bars show the donor levels, with the initial and final charge states labeled in parentheses. Reproduced from [79] with permission from American Physical Society.

is very sensitive to the chemical potential of Zn. This again partly explains that the Zn-rich and Cu-poor condition is beneficial to solar cell efficiencies from the defect perspective.

4. The path towards high-efficiency kesterite solar cell

4.1 Device architecture

The typical device architecture (**Figure 8**) of kesterite-based solar cell inherits from its predecessor chalcopyrite $CuInSe_2$ solar cells due to their similar optical and electronic properties. Metal Mo layer with thickness of 500 nm–1000 nm is usually deposited with sputtering on soda lime glass or other substrates as back contact. Then the kesterite CZTS absorber layer is deposited on top of the Mo layer. The p-n junction is formed by p-type CZTS and the following deposited n-type buffer layer. Typical n-type buffer layer in kesterite and chalcopyrite solar cell is 50 nm–100 nm thick CdS layer usually by chemical bath deposition. Alternative buffer materials such as ZnSnO, Zn(O, S), ZnCdS, etc., have been explored, especially in pure sulfide Cu_2ZnSnS_4 to tackle the unfavorable band alignment found at p-n junction. Next, a 50 nm–100 nm high-resistive intrinsic ZnO (i-ZnO) is deposited.

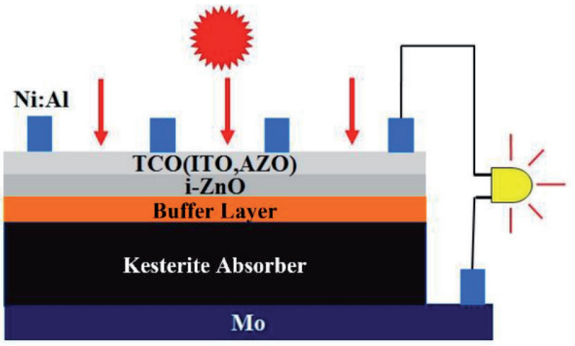

Figure 8.
Schematic device structure of a typical kesterite Cu_2ZnSnS_4 thin film solar cell.

Subsequently, the device structure is completed by deposition of 200 nm–500 nm thick Al-doped ZnO (AZO) or indium tin oxide (ITO) transparent conducting oxide (TCO) layer as the front contact. Ni/Al metal contacts are deposited on the TCO layer for improved current collection. Antireflection coating such as MgF_2 is often deposited on top of the cell to reduce the reflection loss.

Various deposition methods have been investigated for producing high-quality CZTS layer during the development of this technology. These deposition methods are broadly classified as vacuum-based and non-vacuum-based techniques. The vacuum-based methods are usually considered easy to be expanded to commercial scale because of the precise process control. All physical vapor deposition techniques including thermal evaporation, E-beam evaporation [17], sputtering [10, 33, 81, 111], pulsed laser deposition [112] fall into this category. The non-vacuum-based methods are always regarded as low-cost, high-throughput techniques and feasible in roll-to-roll production. These methods usually involve chemical or solution process, such as electrochemical deposition [40], nanoparticle-based synthesis [113, 114], sol–gel spin coating [44, 115], chemical bath deposition (CBD) [116], successive ion layer adsorption and reaction (SILAR) [117], screen printing [118], etc.

4.2 Loss mechanism and solutions

4.2.1 Open-circuit voltage (V_{OC})

In kesterite CZTS solar cells, it has been widely accepted that V_{OC} loss accounts for the majority (more than 50% [119]) of the efficiency gap between the best performance device and the theoretical limit (i.e., Shockley–Queisser radiative limit [120]). V_{OC} loss is determined by the recombination path in the device. The dominant recombination can occur in the bulk of the absorber in the quasi-neutral zone as band-to-band recombination, via defects, or in the space charge region. Another important recombination path can be located at the heterojunction interface between the buffer/window layer and absorber.

Therefore, the absorber problems discussed in **Section 3** such as abundant point defects and defect clusters (i.e., cation disordering), composition variation with narrow stable region are believed to contribute to the recombination. The Cu and Zn substitution with low energy causes a large population of antisite defects such as Cu_{Zn} and Zn_{Cu} and related defects complexes. Consequently, severe electrostatic potential fluctuation and associated band tailing can be observed [121]. In addition, the microinhomogeneities in composition, nonuniform strain, as well as formation of secondary phases lead to band gap fluctuations, which are also detrimental to

V_{OC}. Moreover, acceptor-like Cu_{Zn} defects at the interface will cause Fermi level pinning to a low energy level [122], thus reducing the band bending in the absorber and weakening the electric field. To alleviate the recombination occurring in absorber layer, great efforts have been made over recent years. One solution that has been intensively investigated is cation substitutions because the introduction of larger size cations could result in better cationic ordering, thereby reducing the defects formed because of the Cu and Zn substitution. Using Ag as a substitute for Cu [115], Cd as a substitute for Zn [123, 124], and Ge substitute for Sn [125] are popular choices as they are picked from the same cation groups. As shown in **Figure 9**, Promising progress has been made in this direction both experimentally and theoretically, demonstrating several remarkable efficiencies and mechanism of the defect emerging with cation substitution. Another possible solution to tackle the cationic disorder and related band tailing, as well as to activate the shallower defect is deliberate control of the synthesis condition, for example, post annealing the CZTS absorber within the critical temperature range of 200–250°C and reasonable time range of 1–4 hours will improve the CZTS lattice ordering and increase the band gap [126, 127]. Control of the precursor fabrication process such as the metal stack order, the valence states of the Sn source, has also been reported effective in obtaining less defective absorber and corresponding high-efficiency device [128, 129]. Modification of the sulfurization or selenization condition could also suppress the formation of detrimental intrinsic defects and defect clusters by creating a desirable local chemical environment [11].

In term of the interface recombination path, it is mainly caused by the unpassivated charge defects at the heterojunction and/or the undesirable band alignment between the CZTS absorber and conventional CdS buffer layer. The band alignment problem is more prominent in high band gap pure sulfide Cu_2ZnSnS_4 because of its higher conduction band position. A serious of alternative wide band gap buffer layer materials including ZnCdS [33], Zn(O,S) [130, 131] and ZnSnO [132, 133] have been reported effective in mitigating the band alignment issues. The charge defects at the interface can be reduced by introducing ultrathin layer that has better lattice match with CZTS [10, 81] or alloying Ag near the heterojunction interface to from intrinsic or weak n-type $(Cu,Ag)_2ZnSn(S,Se)_4$ [115, 134]. Dielectric layers have also been investigated for passivating the interface defects, thereby suppressing the interface recombination [111, 135].

4.2.2 Short-circuit current density (J_{SC})

While the V_{OC} loss contributes dominant performance loss in kestrite solar cells, J_{SC} also represents a significant limiting factor for efficiency increases. The J_{SC} loss is mainly caused by two reasons: one is the light or photons that is reflected or absorbed by layers above the CZTS (such as the buffer or window layers as shown in **Figure 8**), which cannot generate electron–hole pairs. The other is the low carrier collection efficiency due to the short diffusion length or narrow depletion width. The first problem can be addressed by introducing antireflection coating and optimizing the optical designs of the top layers above CZTS to increase the fraction of incident light reaching CZTS. The solution has been proven feasible when applying wide band gap buffer layer [111, 133], reducing the thickness and roughness of the top layers [119]. The typical External Quantum Efficiency (EQE) curve of CZTS usually shows relative lack of long wavelength response [9], which might be related to the low carrier lifetime. This low lifetime could also be the results of high defect density in the absorber layer or could simply be a consequence of high recombination loss at the back contact or at the front interface. Therefore, the solutions for suppressing the formation of detrimental defects disused in V_{OC} loss above are also

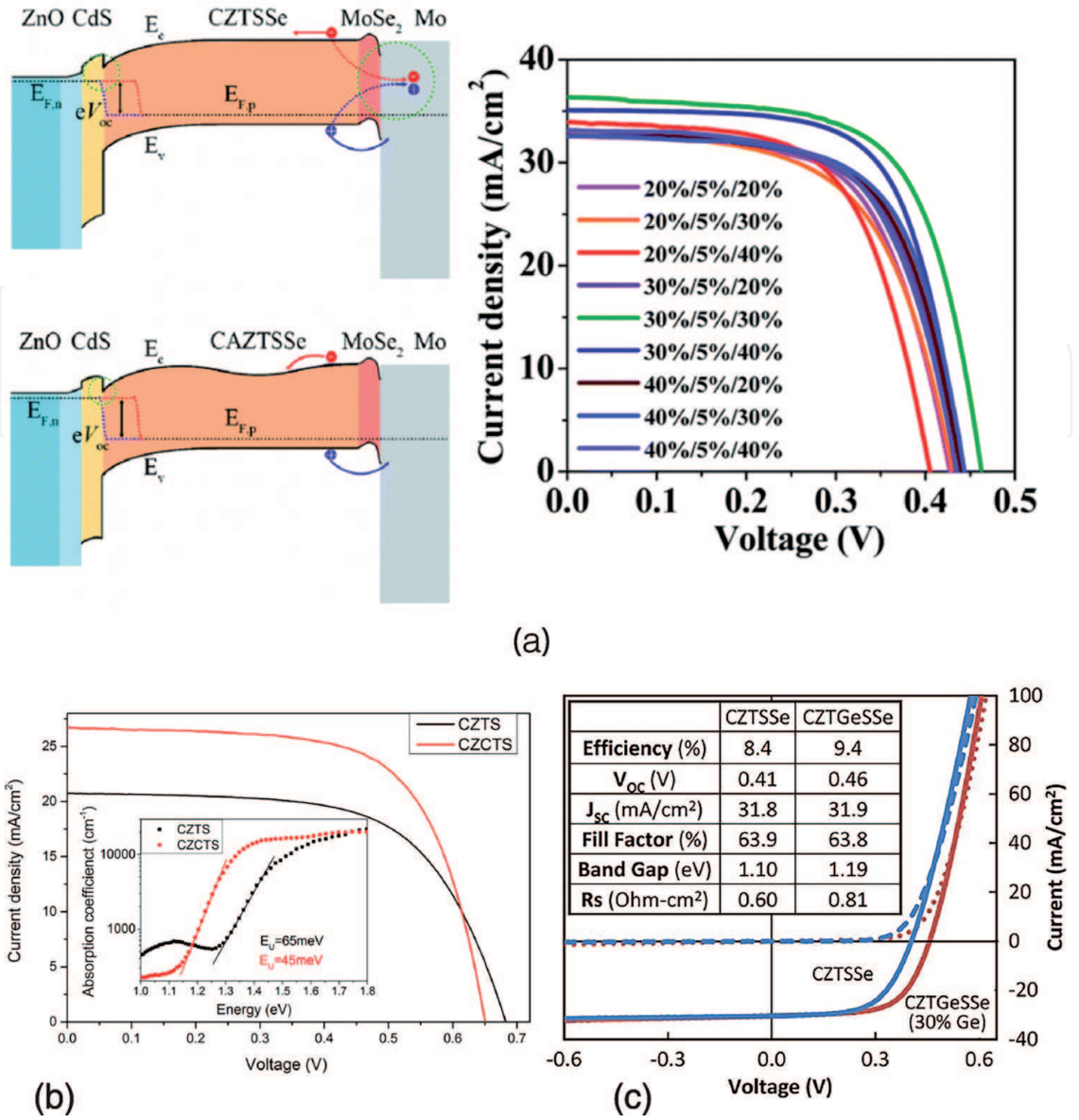

	CZTSSe	CZTGeSSe
Efficiency (%)	8.4	9.4
V_{OC} (V)	0.41	0.46
J_{SC} (mA/cm²)	31.8	31.9
Fill Factor (%)	63.9	63.8
Band Gap (eV)	1.10	1.19
Rs (Ohm-cm²)	0.60	0.81

Figure 9.
(a) The band diagrams of CZTSSe and Ag-graded $(Cu_{1-x}Ag_x)_2ZnSn(S,Se)_4$ (CAZTSSe) solar cells under AM 1.5G 100 mW cm2 illumination and the J–V curves of CAZTSSe solar cells with different Ag composition gradients from the CdS interface to the Mo substrate. (b) J–V curves of CZTS and champion $Cu_2Zn_xCd_{1-x}SnS_4$ (CZCTS) devices and absorption coefficients and Urbach energy (EU) obtained from PDS measurement. (c) J–V curves for the champion CZTSSe and CZTGeSSe (30% Ge) solar cells. Reproduced from [115, 124, 125] with permission from Royal Society of Chemistry, American Chemical Society and John Wiley and Sons.

good for the J_{SC} improvement In addition, band gap grading has also been developed in CZTS to increase the EQE by controlling the [S]/[S + Se] ratio at the surface and back surface [136].

4.2.3 Fill factor (FF)

FF is another significant parameter deficit in kesterite solar cell, which is mainly limited by the series resistance (R_S) in the device. Careful study has been conducted to identify the origin of the R_S, which implies that nonohmic back contact contributes greatly [137]. The nonohmic back contact could be resulted from Schottky barrier formation and/or secondary phase formation at the CZTS/Mo back interface. It is especially severe in high band gap CZTS because of the concentration decrease. Furthermore, the presence of low band gap secondary phases in CZTS could act as shunting pathway, which limits the FF and is therefore undesirable in the device as

well. Deliberate investigation and control of the chemical reaction at the back interface have been proposed to modify the back interface microstructure and improve the device performance including FF [138, 139]. Introducing barrier layer at the CZTS/Mo interface has also been attempted in improving the back interface quality [140, 141].

5. Conclusion

Kesterite CZTS material is an emerging and promising PV technology, which could have the opportunity to realize low-cost and high-volume thin film solar cell production. After undergoing a rapid development in last decades, the technology has attracted increasing attention and demonstrated high potential in high efficiency. Experimental and theoretical studies reveal that the quaternary material exits in kesterite structure, similar to the chalcogenide $CuInS_2$. It has a narrow stable region regarding the chemical potential, which makes the formation of secondary phases very easy. The intrinsic defects characteristic in the CZTS is complex where the deep level antisites defects and defect cluster could be prevalent. These unique properties make it struggling in achieving high-efficiency kesterite solar cells. The sensitive defects environment causes undesirable band tailing, electrostatic potential fluctuations, etc., which become recombination path and limit the open-circuit voltage, as well as other PV performance. The formation of secondary phases can lead to high serious resistance, shunting path depends on the band gap of the phase, which will also limit the device performance. In addition, the heterojunction interface and the Mo/CZTS back interface could also contribute to the performance loss because of the unfavorable band alignment, unpassivated defects, or detrimental reaction during high-temperature annealing. The solutions and approaches for tackling these loss mechanisms have been reviewed at the end of the chapter. Finally, in order to build a successful kesterite CZTS technology, combining the advanced approaches summarized in this chapter with further exploring the material synthesis and device physics would pave a path for higher efficiency.

Acknowledgements

This work was supported by the National Key R&D Program of China (No. 2018YFE0203400), the Science and Technology Innovation Program of Hunan Province (No. 2020RC2005), Australian Renewable Energy Agency (ARENA, 2017/RND006), and International Postdoctoral Exchange Fellowship Program (YJ20200207). X.H. acknowledges Australian Research Council (ARC) Future Fellowship (FT190100756). K.S. acknowledges the support from Australian Government through the Australian Renewable Energy Agency (ARENA) and the Australian Centre of Advanced Photovoltaics (ACAP, Grant No.1-SRI001).

Conflict of interest

The authors declare no conflict of interest.

DOI: http://dx.doi.org/10.5772/intechopen.101744

Author details

Kaiwen Sun[1,2*], Fangyang Liu[1*] and Xiaojing Hao[2*]

1 School of Metallurgy and Environment, Central South University, Changsha, China

2 Australian Centre for Advanced Photovoltaics, School of Photovoltaic and Renewable Energy Engineering, University of New South Wales, Sydney, Australia

*Address all correspondence to: kaiwen.sun@unsw.edu.au, liufangyang@csu.edu.cn and xj.hao@unsw.edu.au

References

[1] Nakamura M, Yamaguchi K, Kimoto Y, Yasaki Y, Kato T, Sugimoto H. Cd-Free Cu(In,Ga)(Se,S)$_2$ thin-film solar cell with record efficiency of 23.35%. IEEE Journal of Photovoltaics. 2019;**9**(6):1863-1867. DOI: 10.1109/JPHOTOV.2019.2937218

[2] Green MA, Dunlop ED, Hohl-Ebinger J, Yoshita M, Kopidakis N, Hao X. Solar cell efficiency tables (Version 58). Progress in Photovoltaics: Research and Applications. 2021;**29**(7):657-667. DOI: 10.1002/pip.3444

[3] Commission E. Restriction of Hazardous Substances in Electrical and Electronic Equipment (RoHS). Strasbourg: European Commission; 2011 Available from: https://ec.europa.eu/environment/topics/waste-and-recycling/rohs-directive_en#ecl-inpage-622

[4] Commission E. Critical Raw Materials. Brussels: European Commission; 2011 Available from: https://ec.europa.eu/growth/sectors/raw-materials/areas-specific-interest/critical-raw-materials_en

[5] Walsh A, Chen S, Wei S-H, Gong X-G. Kesterite thin-film solar cells: Advances in materials modelling of Cu2ZnSnS4. Advanced Energy Materials. 2012;**2**(4):400-409. DOI: 10.1002/aenm.201100630

[6] Zhou H, Hsu W-C, Duan H-S, Bob B, Yang W, Song T-B, et al. CZTS nanocrystals: A promising approach for next generation thin film photovoltaics. Energy & Environmental Science. 2013;**6**(10):2822-2838. DOI: 10.1039/C3EE41627E

[7] Ito K. An overview of CZTS-based thin-film solar cells. In: Copper Zinc Tin Sulfide-Based Thin-Film Solar Cells. West Sussex, United Kingdom: John Wiley & Sons, Ltd.; 2014. pp. 1-41

[8] Katagiri H, Jimbo K, Maw WS, Oishi K, Yamazaki M, Araki H, et al. Development of CZTS-based thin film solar cells. Thin Solid Films. 2009;**517**(7):2455-2460. DOI: 10.1016/j.tsf.2008.11.002

[9] Mitzi DB, Gunawan O, Todorov TK, Wang K, Guha S. The path towards a high-performance solution-processed kesterite solar cell. Solar Energy Materials and Solar Cells. 2011;**95**(6):1421-1436. DOI: 10.1016/j.solmat.2010.11.028

[10] Yan C, Huang J, Sun K, Johnston S, Zhang Y, Sun H, et al. Cu2ZnSnS4 solar cells with over 10% power conversion efficiency enabled by heterojunction heat treatment. Nature Energy. 2018;**3**(9):764-772. DOI: 10.1038/s41560-018-0206-0

[11] Li J, Huang Y, Huang J, Liang G, Zhang Y, Rey G, et al. Defect control for 12.5% efficiency Cu2ZnSnSe4 Kesterite thin-film solar cells by Engineering of local chemical environment. Advanced Materials. 2020;**32**(52):2005268. DOI: 10.1002/adma.202005268

[12] NREL. Best Research-Cell Efficiency Chart. Golden, United States: The National Renewable Energy Laboratory; 2021 Available from: https://www.nrel.gov/pv/cell-efficiency.html.

[13] Nitsche R, Sargent DF, Wild P. Crystal growth of quaternary 122464 chalcogenides by iodine vapor transport. Journal of Crystal Growth. 1967;**1**(1):52-53. DOI: 10.1016/0022-0248(67)90009-7

[14] Ito K, Nakazawa T. Electrical and optical properties of Stannite-type quaternary semiconductor thin films. Japanese Journal of Applied Physics. 1988;**27**(Part 1, No 11):2094-2097. DOI: 10.1143/jjap.27.2094

[15] Ito K, Nakazawa T. Stannite-type photovoltaic thin films. In: Proceedings

of the 4th International Conference of Photovoltaic Science and Engineering. Sydney, NSW Australia: Institution of Radio and Electronics Engineers Australia; 1989

[16] Katagiri H, Sasaguchi N, Hando S, Hoshino S, Ohashi J, Yokota T. Preparation and evaluation of Cu_2ZnSnS_4 thin films by sulfurization of E-B evaporated precursor. In: Technical Digest of the 9th International Conference of Photovoltaic Science and Engineering. Miyazaki, Japan: PVSEC-9; 1996

[17] Katagiri H, Sasaguchi N, Hando S, Hoshino S, Ohashi J, Yokota T. Preparation and evaluation of Cu2ZnSnS4 thin films by sulfurization of E·B evaporated precursors. Solar Energy Materials and Solar Cells. 1997;**49**(1):407-414. DOI: 10.1016/S0927-0248(97)00119-0

[18] Friedlmeier TM, Wieser N, Walter T, Dittrich H, Schock H. Heterojunctions based on Cu2ZnSnS4 and Cu2ZnSnSe4 thin films. In: Proceedings of the 14th European Conference of Photovoltaic Science and Engineering and Exhibition. Barcelona, Spain: European Photovoltaic Solar Energy Conference; 1997

[19] Katagiri H. Cu2ZnSnS4 thin film solar cells. Thin Solid Films. 2005; **480-481**:426-432. DOI: 10.1016/j.tsf.2004.11.024

[20] Katagiri H, Ishigaki N, Ishida T, Saito K. Characterization of Cu2ZnSnS4 thin films prepared by vapor phase sulfurization. Japanese Journal of Applied Physics. 2001;**40**(Part 1, No. 2A):500-504.DOI: 10.1143/jjap.40.500

[21] Katagiri H, Saitoh K, Washio T, Shinohara H, Kurumadani T, Miyajima S. Development of thin film solar cell based on Cu2ZnSnS4 thin films. Solar Energy Materials and Solar Cells. 2001;**65**(1):141-148. DOI: 10.1016/S0927-0248(00)00088-X

[22] Katagiri H, Jimbo K, Moriya K, Tsuchida K, editors. Solar cell without environmental pollution by using CZTS thin film. 3rd World Conference on Photovoltaic Energy Conversion. Osaka, Japan: IEEE; 2003

[23] Kobayashi T, Jimbo K, Tsuchida K, Shinoda S, Oyanagi T, Katagiri H. Investigation of Cu2ZnSnS4-based thin film solar cells using abundant materials. Japanese Journal of Applied Physics. 2005;**44**(1B):783-787. DOI: 10.1143/jjap.44.783

[24] Jimbo K, Kimura R, Kamimura T, Yamada S, Maw WS, Araki H, et al. Cu2ZnSnS4-type thin film solar cells using abundant materials. Thin Solid Films. 2007;**515**(15):5997-5999. DOI: 10.1016/j.tsf.2006.12.103

[25] Katagiri H, Jimbo K, Yamada S, Kamimura T, Maw WS, Fukano T, et al. Enhanced conversion efficiencies of Cu2ZnSnS4-based thin film solar cells by using preferential etching technique. Applied Physics Express. 2008;**1**:041201. DOI: 10.1143/apex.1.041201

[26] Tajima S, Itoh T, Hazama H, Ohishi K, Asahi R. Improvement of the open-circuit voltage of Cu_2ZnSnS_4 cells using a two-layered process. In: IEEE 40th Photovoltaic Specialist Conference (PVSC). Denver, CO, USA: IEEE; 2014. DOI: 10.1109/PVSC.2014.6924951

[27] Todorov TK, Reuter KB, Mitzi DB. High-efficiency solar cell with Earth-abundant liquid-processed absorber. Advanced Materials. 2010;**22**(20):E156-E1E9. DOI: 10.1002/adma.200904155

[28] Repins I, Beall C, Vora N, DeHart C, Kuciauskas D, Dippo P, et al. Co-evaporated Cu2ZnSnSe4 films and devices. Solar Energy Materials and Solar Cells. 2012;**101**:154-159. DOI: 10.1016/j.solmat.2012.01.008

[29] Sugimoto H, Liao C, Hiroi H, Sakai N, Kato T. Lifetime improvement

for high efficiency Cu_2ZnSnS_4 submodules. In: IEEE 39th Photovoltaic Specialists Conference (PVSC). Tampa, FL, USA: IEEE; 2013. DOI: 10.1109/PVSC.2013.6745135

[30] Haass SG, Diethelm M, Werner M, Bissig B, Romanyuk YE, Tiwari AN. 11.2% Efficient solution processed Kesterite solar cell with a low voltage deficit. Advanced Energy Materials. 2015;**5**(18):1500712(1-7). DOI: 10.1002/aenm.201500712

[31] Lin X, Kavalakkatt J, Lux-Steiner MC, Ennaoui A. Inkjet-printed Cu2ZnSn(S, Se)4 solar cells. Advanced Science. 2015;**2**:1500028(1-6). DOI: 10.1002/advs.201500028

[32] Schnabel T, Abzieher T, Friedlmeier TM, Ahlswede E. Solution-based preparation of Cu2ZnSn(S,Se)4 for solar cells—Comparison of SnSe2 and elemental Se as Chalcogen source. IEEE Journal of Photovoltaics. 2015;**5**(2):670-675. DOI: 10.1109/JPHOTOV.2015.2392935

[33] Sun K, Yan C, Liu F, Huang J, Zhou F, Stride JA, et al. Over 9% efficient Kesterite Cu2ZnSnS4 solar cell fabricated by using Zn1–xCdxS buffer layer. Advanced Energy Materials. 2016;**6**(12):1600046. DOI: 10.1002/aenm.201600046

[34] Barkhouse DAR, Gunawan O, Gokmen T, Todorov TK, Mitzi DB. Device characteristics of a 10.1% hydrazine-processed Cu2ZnSn(Se,S)4 solar cell. Progress in Photovoltaics: Research and Applications. 2012;**20**(1):6-11. DOI: 10.1002/pip.1160

[35] Qijie G, Yanyan C, Caspar JV, Farneth WE, Ionkin AS, Johnson LK, et al. A simple solution-based route to high-efficiency CZTSSe thin-film solar cells. In: Photovoltaic Specialists Conference (PVSC), 2012 38th IEEE. Austin, TX, USA: IEEE; 2012. DOI: 10.1109/PVSC.2012.6318213

[36] Yang W, Duan H-S, Bob B, Zhou H, Lei B, Chung C-H, et al. Novel solution processing of high-efficiency Earth-abundant Cu2ZnSn(S,Se)4 solar cells. Advanced Materials. 2012;**24**(47):6323-6329. DOI: 10.1002/adma.201201785

[37] Xin H, Katahara JK, Braly IL, Hillhouse HW. 8% Efficient Cu2ZnSn(S,Se)4 solar cells from redox equilibrated simple precursors in DMSO. Advanced Energy Materials. 2014;**4**(11):1301823 (1-5). DOI: 10.1002/aenm.201301823

[38] Shin B, Gunawan O, Zhu Y, Bojarczuk NA, Chey SJ, Guha S. Thin film solar cell with 8.4% power conversion efficiency using an earth-abundant Cu2ZnSnS4 absorber. Progress in Photovoltaics: Research and Applications. 2013;**21**(1):72-76. DOI: 10.1002/pip.1174

[39] Wang W, Winkler MT, Gunawan O, Gokmen T, Todorov TK, Zhu Y, et al. Device characteristics of CZTSSe thin-film solar cells with 12.6% efficiency. Advanced Energy Materials. 2014;**4**(7): 1301465 (1-5). DOI: 10.1002/aenm.201301465

[40] Ahmed S, Reuter KB, Gunawan O, Guo L, Romankiw LT, Deligianni H. A high efficiency electrodeposited Cu2ZnSnS4 solar cell. Advanced Energy Materials. 2012;**2**(2):253-259. DOI: 10.1002/aenm.201100526

[41] Todorov TK, Tang J, Bag S, Gunawan O, Gokmen T, Zhu Y, et al. Beyond 11% efficiency: Characteristics of state-of-the-art Cu2ZnSn(S,Se)4 solar cells. Advanced Energy Materials. 2012;**2013**:34-38. DOI: 10.1002/aenm.201200348

[42] Yang K-J, Son D-H, Sung S-J, Sim J-H, Kim Y-I, Park S-N, et al. A band-gap-graded CZTSSe solar cell with 12.3% efficiency. Journal of Materials Chemistry A. 2016;**4**(26):10151-10158. DOI: 10.1039/C6TA01558A

[43] Son D-H, Kim S-H, Kim S-Y, Kim Y-I, Sim J-H, Park S-N, et al. Effect of solid-H2S gas reactions on CZTSSe thin film growth and photovoltaic properties of a 12.62% efficiency device. Journal of Materials Chemistry A. 2019;**7**(44): 25279-25289. DOI: 10.1039/C9TA08310C

[44] Su Z, Liang G, Fan P, Luo J, Zheng Z, Xie Z, et al. Device postannealing enabling over 12% efficient solution-processed Cu2ZnSnS4 solar cells with Cd2+ substitution. Advanced Materials. 2020;**32**(32): 2000121. DOI: 10.1002/adma.202000121

[45] Du Y, Wang S, Tian Q, Zhao Y, Chang X, Xiao H, et al. Defect Engineering in Earth-abundant Cu2ZnSn(S,Se)4 photovoltaic materials via Ga3+-doping for over 12% efficient solar cells. Advanced Functional Materials. 2021;**31**(16):2010325. DOI: 10.1002/adfm.202010325

[46] Gong Y, Qiu R, Niu C, Fu J, Jedlicka E, Giridharagopal R, et al. Ag Incorporation with controlled grain growth enables 12.5% efficient Kesterite solar cell with open circuit voltage reached 64.2% Shockley–Queisser limit. Advanced Functional Materials. 2021;**31**(24):2101927. DOI: 10.1002/adfm.202101927

[47] Chen S, Gong XG, Walsh A, Wei S-H. Electronic structure and stability of quaternary chalcogenide semiconductors derived from cation cross-substitution of II-VI and I-III-VI compounds. Physical Review B. 2009;**79**(16):165211. DOI: 10.1103/PhysRevB.79.165211

[48] Chen S, Gong XG, Walsh A, Wei S-H. Crystal and electronic band structure of Cu2ZnSnX4 (X=S and Se) photovoltaic absorbers: First-principles insights. Applied Physics Letters. 2009;**94**(4):041903. DOI: 10.1063/1.3074499

[49] Hall S, Szymanski J, Stewart J. Kesterite, (Cu< 2)(Zn, Fe) SnS< 4), and stannite, Cu< 2)(Fe, Zn) SnS< 4), structurally similar but distinct minerals. The Canadian Mineralogist. 1978;**16**(2):131-137

[50] Schorr S, Hoebler H-J, Tovar M. A neutron diffraction study of the stannite-kesterite solid solution series. European Journal of Mineralogy. 2007;**19**(1):65-73. DOI: 10.1127/0935-1221/2007/0019-0065

[51] Friedelmeier T, Dittrich H, Schock H-W. Growth and characterization of Cu2ZnSnS4 and Cu2ZnSnSe4 thin films for photovoltaic applications. In: Ternary and Multinary Compounds. University of Salford, UK: CRC Press; 1998. p. 345

[52] Bernardini GP, Borrini D, Caneschi A, Di Benedetto F, Gatteschi D, Ristori S, et al. EPR and SQUID magnetometry study of Cu2FeSnS4 (stannite) and Cu2ZnSnS4 (kesterite). Physics and Chemistry of Minerals. 2000;**27**(7):453-461. DOI: 10.1007/s002690000086

[53] Schorr S. The crystal structure of kesterite type compounds: A neutron and X-ray diffraction study. Solar Energy Materials and Solar Cells. 2011;**95**(6):1482-1488. DOI: 10.1016/j.solmat.2011.01.002

[54] Hall S, Kissin S, Stewart J. Stannite and kesterite-distinct minerals or components of a solid-solution. In: Acta crystallographica section A. Copenhagen, Denmark: Munksgaard Int Publ Ltd.; Vol. 31. 1975 p. s67

[55] Seol J-S, Lee S-Y, Lee J-C, Nam H-D, Kim K-H. Electrical and optical properties of Cu2ZnSnS4 thin films prepared by rf magnetron sputtering process. Solar Energy Materials and Solar Cells. 2003;**75**(1):155-162. DOI: 10.1016/S0927-0248(02)00127-7

[56] Babu GS, Kumar YBK, Bhaskar PU, Raja VS. Effect of post-deposition annealing on the growth of

Cu2ZnSnSe4 thin films for a solar cell absorber layer. Semiconductor Science and Technology. 2008;**23**(8):085023. DOI: 10.1088/0268-1242/23/8/085023

[57] Chen S, Walsh A, Luo Y, Yang J-H, Gong XG, Wei S-H. Wurtzite-derived polytypes of kesterite and stannite quaternary chalcogenide semiconductors. Physical Review B. 2010;**82**(19):195203. DOI: 10.1103/PhysRevB.82.195203

[58] Paier J, Asahi R, Nagoya A, Kresse G. Cu_2ZnSnS_4 as a potential photovoltaic material: A hybrid Hartree-Fock density functional theory study. Physical Review B. 2009;**79**(11):115126. DOI: 10.1103/PhysRevB.79.115126

[59] Persson C. Electronic and optical properties of Cu2ZnSnS4 and Cu2ZnSnSe4. Journal of Applied Physics. 2010;**107**(5):053710. DOI: 10.1063/1.3318468

[60] Schorr S. Structural aspects of adamantine like multinary chalcogenides. Thin Solid Films. 2007;**515**(15):5985-5991. DOI: 10.1016/j.tsf.2006.12.100

[61] Botti S, Kammerlander D, Marques MAL. Band structures of Cu2ZnSnS4 and Cu2ZnSnSe4 from many-body methods. Applied Physics Letters. 2011;**98**(24):241915. DOI: 10.1063/1.3600060

[62] Ichimura M, Nakashima Y. Analysis of atomic and electronic structures of Cu2ZnSnS4 based on first-principle calculation. Japanese Journal of Applied Physics. 2009;**48**(9):090202. DOI: 10.1143/jjap.48.090202

[63] Persson C, Chen R, Zhao H, Kumar M, Huang D. Electronic Structure and Optical Properties from First-Principles Modeling. In: Copper Zinc Tin Sulfide-Based Thin-Film Solar Cells. West Sussex, United Kingdom: John Wiley & Sons, Ltd.; 2014. pp. 75-105

[64] Nakayama N, Ito K. Sprayed films of stannite Cu2ZnSnS4. Applied Surface Science. 1996;**92**:171-175. DOI: 10.1016/0169-4332(95)00225-1

[65] Kamoun N, Bouzouita H, Rezig B. Fabrication and characterization of Cu2ZnSnS4 thin films deposited by spray pyrolysis technique. Thin Solid Films. 2007;**515**(15):5949-5952. DOI: 10.1016/j.tsf.2006.12.144

[66] Gao F, Yamazoe S, Maeda T, Nakanishi K, Wada T. Structural and optical properties of In-free Cu2ZnSn(S,Se)4 solar cell materials. Japanese Journal of Applied Physics. 2012;**51**:10NC29. DOI: 10.1143/jjap.51.10nc29

[67] Tanaka K, Fukui Y, Moritake N, Uchiki H. Chemical composition dependence of morphological and optical properties of Cu2ZnSnS4 thin films deposited by sol–gel sulfurization and Cu2ZnSnS4 thin film solar cell efficiency. Solar Energy Materials and Solar Cells. 2011;**95**(3):838-842. DOI: 10.1016/j.solmat.2010.10.031

[68] Patel M, Mukhopadhyay I, Ray A. Structural, optical and electrical properties of spray-deposited CZTS thin films under a non-equilibrium growth condition. Journal of Physics D: Applied Physics. 2012;**45**(44):445103. DOI: 10.1088/0022-3727/45/44/445103

[69] Ahn S, Jung S, Gwak J, Cho A, Shin K, Yoon K, et al. Determination of band gap energy (Eg) of Cu2ZnSnSe4 thin films: On the discrepancies of reported band gap values. Applied Physics Letters. 2010;**97**(2):021905. DOI: 10.1063/1.3457172

[70] Haight R, Barkhouse A, Gunawan O, Shin B, Copel M, Hopstaken M, et al. Band alignment at the Cu2ZnSn(SxSe1−x)4/CdS interface. Applied Physics Letters. 2011;**98**(25):253502. DOI: 10.1063/1.3600776

[71] He J, Sun L, Chen S, Chen Y, Yang P, Chu J. Composition dependence of

structure and optical properties of Cu2ZnSn(S,Se)4 solid solutions: An experimental study. Journal of Alloys and Compounds. 2012;**511**(1):129-132. DOI: 10.1016/j.jallcom.2011.08.099

[72] Ennaoui A, Lux-Steiner M, Weber A, Abou-Ras D, Kötschau I, Schock HW, et al. Cu2ZnSnS4 thin film solar cells from electroplated precursors: Novel low-cost perspective. Thin Solid Films. 2009;**517**(7):2511-2514. DOI: 10.1016/j.tsf.2008.11.061

[73] Kumar M, Zhao H, Persson C. Cation vacancies in the alloy compounds of Cu2ZnSn(S1−xSex)4 and CuIn(S1−xSex)2. Thin Solid Films. 2013;**535**:318-321. DOI: 10.1016/j.tsf.2012.11.063

[74] Chen S, Walsh A, Gong X-G, Wei S-H. Classification of lattice defects in the Kesterite Cu2ZnSnS4 and Cu2ZnSnSe4 Earth-abundant solar cell absorbers. Advanced Materials. 2013;**25**(11):1522-1539. DOI: 10.1002/adma.201203146

[75] Lund EA, Du H, Hlaing Oo WM, Teeter G, Scarpulla MA. Investigation of combinatorial coevaporated thin film Cu2ZnSnS4 (II): Beneficial cation arrangement in Cu-rich growth. Journal of Applied Physics. 2014;**115**(17):173503. DOI: 10.1063/1.4871665

[76] Chen S, Gong XG, Walsh A, Wei S-H. Defect physics of the kesterite thin-film solar cell absorber Cu2ZnSnS4. Applied Physics Letters. 2010;**96**(2):021902. DOI: 10.1063/1.3275796

[77] Olekseyuk ID, Dudchak IV, Piskach LV. Phase equilibria in the Cu2S–ZnS–SnS2 system. Journal of Alloys and Compounds. 2004;**368**(1):135-143. DOI: 10.1016/j.jallcom.2003.08.084

[78] Dudchak IV, Piskach LV. Phase equilibria in the Cu2SnSe3–SnSe2–ZnSe system. Journal of Alloys and Compounds. 2003;**351**(1):145-150. DOI: 10.1016/S0925-8388(02)01024-1

[79] Chen S, Yang J-H, Gong XG, Walsh A, Wei S-H. Intrinsic point defects and complexes in the quaternary kesterite semiconductor Cu_2ZnSnS_4. Physical Review B. 2010;**81**(24):245204. DOI: 10.1103/PhysRevB.81.245204

[80] Siebentritt S, Schorr S. Kesterites—a challenging material for solar cells. Progress in Photovoltaics: Research and Applications. 2012;**20**(5):512-519. DOI: 10.1002/pip.2156

[81] Sun K, Huang J, Yan C, Pu A, Liu F, Sun H, et al. Self-assembled nanometer-scale ZnS structure at the CZTS/ZnCdS heterointerface for high-efficiency wide band gap Cu2ZnSnS4 solar cells. Chemistry of Materials. 2018;**30**(12):4008-4016. DOI: 10.1021/acs.chemmater.8b00009

[82] Berg DM, Djemour R, Gütay L, Zoppi G, Siebentritt S, Dale PJ. Thin film solar cells based on the ternary compound Cu2SnS3. Thin Solid Films. 2012;**520**(19):6291-6294. DOI: 10.1016/j.tsf.2012.05.085

[83] Marcano G, Rincón C, de Chalbaud LM, Bracho DB, Pérez GS. Crystal growth and structure, electrical, and optical characterization of the semiconductor Cu2SnSe3. Journal of Applied Physics. 2001;**90**(4):1847-1853. DOI: 10.1063/1.1383984

[84] Yu P, Cardona M. Fundamentals of Semiconductors. 4th ed. Berlin, Heidelberg, Germany: Springer; 2010

[85] Lin Y-T, Shi J-B, Chen Y-C, Chen C-J, Wu P-F. Synthesis and characterization of Tin Disulfide (SnS2) nanowires. Nanoscale Research Letters. 2009;**4**(7):694. DOI: 10.1007/s11671-009-9299-5

[86] Sava F, Lörinczi A, Popescu M, Socol G, Axente E, Mihailescu IN, et al. Amorphous SnSe2 films. Journal of Optoelectronics and Advanced Materials. 2006;**8**(4):1367-1371

[87] Vidal J, Lany S, d'Avezac M, Zunger A, Zakutayev A, Francis J, et al. Band-structure, optical properties, and defect physics of the photovoltaic semiconductor SnS. Applied Physics Letters. 2012;**100**(3):032104. DOI: 10.1063/1.3675880

[88] Sinsermsuksakul P, Heo J, Noh W, Hock AS, Gordon RG. Atomic layer deposition of Tin monosulfide thin films. Advanced Energy Materials. 2011;**1**(6):1116-1125. DOI: 10.1002/aenm.201100330

[89] Franzman MA, Schlenker CW, Thompson ME, Brutchey RL. Solution-phase synthesis of SnSe nanocrystals for use in solar cells. Journal of the American Chemical Society. 2010;**132**(12): 4060-4061. DOI: 10.1021/ja100249m

[90] Liu G, Schulmeyer T, Brötz J, Klein A, Jaegermann W. Interface properties and band alignment of Cu2S/CdS thin film solar cells. Thin Solid Films. 2003;**431-432**:477-482. DOI: 10.1016/S0040-6090(03)00190-1

[91] Kashida S, Shimosaka W, Mori M, Yoshimura D. Valence band photoemission study of the copper chalcogenide compounds, Cu2S, Cu2Se and Cu2Te. Journal of Physics and Chemistry of Solids. 2003;**12**:2357-2363. DOI: 10.1016/S0022-3697(03)00272-5

[92] Siebentritt S. Why are kesterite solar cells not 20% efficient? Thin Solid Films. 2013;**535**:1-4. DOI: 10.1016/j.tsf.2012.12.089

[93] Timo Wätjen J, Engman J, Edoff M, Platzer-Björkman C. Direct evidence of current blocking by ZnSe in Cu2ZnSnSe4 solar cells. Applied Physics Letters. 2012;**100**(17):173510. DOI: 10.1063/1.4706256

[94] Redinger A, Mousel M, Wolter MH, Valle N, Siebentritt S. Influence of S/Se ratio on series resistance and on dominant recombination pathway in Cu2ZnSn(SSe)4 thin film solar cells. Thin Solid Films. 2013;**535**:291-295. DOI: 10.1016/j.tsf.2012.11.111

[95] Mendis BG, Goodman MCJ, Major JD, Taylor AA, Durose K, Halliday DP. The role of secondary phase precipitation on grain boundary electrical activity in Cu2ZnSnS4 (CZTS) photovoltaic absorber layer material. Journal of Applied Physics. 2012;**112**(12):124508. DOI: 10.1063/1.4769738

[96] Sun K, Yan C, Huang J, Liu F, Li J, Sun H, et al. Beyond 10% efficiency Cu2ZnSnS4 solar cells enabled by modifying the heterojunction interface chemistry. Journal of Materials Chemistry A. 2019;**7**(48):27289-27296. DOI: 10.1039/C9TA09576D

[97] Redinger A, Siebentritt S. Coevaporation of Cu2ZnSnSe4 thin films. Applied Physics Letters. 2010;**97**(9):092111. DOI: 10.1063/1.3483760

[98] Mousel M, Redinger A, Djemour R, Arasimowicz M, Valle N, Dale P, et al. HCl and Br2-MeOH etching of Cu2ZnSnSe4 polycrystalline absorbers. Thin Solid Films. 2013;**535**:83-87. DOI: 10.1016/j.tsf.2012.12.095

[99] Nagoya A, Asahi R, Wahl R, Kresse G. Defect formation and phase stability of Cu2ZnSnS4 photovoltaic material. Physical Review B. 2010;**81**(11):113202. DOI: 10.1103/PhysRevB.81.113202

[100] Wibowo RA, Kim WS, Lee ES, Munir B, Kim KH. Single step preparation of quaternary Cu2ZnSnSe4 thin films by RF magnetron sputtering from binary chalcogenide targets. Journal of Physics and Chemistry of Solids. 2007;**68**(10):1908-1913. DOI: 10.1016/j.jpcs.2007.05.022

[101] Zhang X, Shi X, Ye W, Ma C, Wang C. Electrochemical deposition of quaternary Cu2ZnSnS4 thin films as potential solar cell material. Applied Physics A. 2009;**94**(2):381-386. DOI: 10.1007/s00339-008-4815-5

[102] Tanaka T, Nagatomo T, Kawasaki D, Nishio M, Guo Q, Wakahara A, et al. Preparation of Cu2ZnSnS4 thin films by hybrid sputtering. Journal of Physics and Chemistry of Solids. 2005;**66**(11):1978-1981. DOI: 10.1016/j.jpcs.2005.09.037

[103] Scragg JJ, Dale PJ, Peter LM, Zoppi G, Forbes I. New routes to sustainable photovoltaics: evaluation of Cu2ZnSnS4 as an alternative absorber material. Physica Status Solidi (b). 2008;**245**(9):1772-1778. DOI: 10.1002/pssb.200879539

[104] Altosaar M, Raudoja J, Timmo K, Danilson M, Grossberg M, Krustok J, et al. Cu2Zn1–x Cdx Sn(Se1–y Sy)4 solid solutions as absorber materials for solar cells. Physica Status Solidi (a). 2008;**205**(1):167-170. DOI: 10.1002/pssa.200776839

[105] Oishi K, Saito G, Ebina K, Nagahashi M, Jimbo K, Maw WS, et al. Growth of Cu2ZnSnS4 thin films on Si (100) substrates by multisource evaporation. Thin Solid Films. 2008;**517**(4):1449-1452. DOI: 10.1016/j.tsf.2008.09.056

[106] Kishore Kumar YB, Suresh Babu G, Uday Bhaskar P, Sundara RV. Preparation and characterization of spray-deposited Cu2ZnSnS4 thin films. Solar Energy Materials and Solar Cells. 2009;**93**(8):1230-1237. DOI: 10.1016/j.solmat.2009.01.011

[107] Hönes K, Zscherpel E, Scragg J, Siebentritt S. Shallow defects in Cu2ZnSnS4. Physica B: Condensed Matter. 2009;**404**(23):4949-4952. DOI: 10.1016/j.physb.2009.08.206

[108] Shinde NM, Dubal DP, Dhawale DS, Lokhande CD, Kim JH, Moon JH. Room temperature novel chemical synthesis of Cu2ZnSnS4 (CZTS) absorbing layer for photovoltaic application. Materials Research Bulletin. 2012;**47**(2):302-307. DOI: 10.1016/j.materresbull.2011.11.020

[109] Miyamoto Y, Tanaka K, Oonuki M, Moritake N, Uchiki H. Optical properties of Cu2ZnSnS4 thin films prepared by Sol–Gel and sulfurization method. Japanese Journal of Applied Physics. 2008;**47**(1):596-597. DOI: 10.1143/jjap.47.596

[110] Prabhakar T, Jampana N. Effect of sodium diffusion on the structural and electrical properties of Cu2ZnSnS4 thin films. Solar Energy Materials and Solar Cells. 2011;**95**(3):1001-1004. DOI: 10.1016/j.solmat.2010.12.012

[111] Cui X, Sun K, Huang J, Yun JS, Lee C-Y, Yan C, et al. Cd-Free Cu2ZnSnS4 solar cell with an efficiency greater than 10% enabled by Al2O3 passivation layers. Energy & Environmental Science. 2019;**12**(9):2751-2764. DOI: 10.1039/C9EE01726G

[112] Cazzaniga A, Crovetto A, Yan C, Sun K, Hao X, Ramis Estelrich J, et al. Ultra-thin Cu2ZnSnS4 solar cell by pulsed laser deposition. Solar Energy Materials and Solar Cells. 2017;**166**:91-99. DOI: 10.1016/j.solmat.2017.03.002

[113] Guo Q, Ford GM, Yang W-C, Walker BC, Stach EA, Hillhouse HW, et al. Fabrication of 7.2% Efficient CZTSSe Solar Cells Using CZTS Nanocrystals. Journal of the American Chemical Society. 2010;**132**(49):17384-17386. DOI: 10.1021/ja108427b

[114] Cao Y, Denny MS, Caspar JV, Farneth WE, Guo Q, Ionkin AS, et al. High-efficiency solution-processed Cu2ZnSn(S,Se)4 thin-film solar cells prepared from binary and ternary nanoparticles. Journal of the American Chemical Society. 2012;**134**(38):15644-15647. DOI: 10.1021/ja3057985

[115] Qi Y-F, Kou D-X, Zhou W-H, Zhou Z-J, Tian Q-W, Meng Y-N, et al. Engineering of interface band bending and defects elimination via a Ag-graded active layer for efficient

(Cu,Ag)2ZnSn(S,Se)4 solar cells. Energy & Environmental Science. 2017;**10**(11):2401-2410. DOI: 10.1039/C7EE01405H

[116] Wangperawong A, King JS, Herron SM, Tran BP, Pangan-Okimoto K, Bent SF. Aqueous bath process for deposition of Cu2ZnSnS4 photovoltaic absorbers. Thin Solid Films. 2011;**519**(8):2488-2492. DOI: 10.1016/j.tsf.2010.11.040

[117] Sun K, Wang A, Su Z, Liu F, Hao X. Enhancing the performance of Cu2ZnSnS4 solar cell fabricated via successive ionic layer adsorption and reaction method by optimizing the annealing process. Solar Energy. 2021;**220**:204-210. DOI: 10.1016/j.solener.2021.03.033

[118] Zhou Z, Wang Y, Xu D, Zhang Y. Fabrication of Cu2ZnSnS4 screen printed layers for solar cells. Solar Energy Materials and Solar Cells. 2010;**94**(12):2042-2045. DOI: 10.1016/j.solmat.2010.06.010

[119] Winkler MT, Wang W, Gunawan O, Hovel HJ, Todorov TK, Mitzi DB. Optical designs that improve the efficiency of Cu2ZnSn(S,Se)4 solar cells. Energy & Environmental Science. 2014;**7**(3):1029-1036. DOI: 10.1039/C3EE42541J

[120] Shockley W, Queisser HJ. Detailed balance limit of efficiency of p-n junction solar cells. Journal of Applied Physics. 1961;**32**(3):510-519. DOI: 10.1063/1.1736034

[121] Gokmen T, Gunawan O, Todorov TK, Mitzi DB. Band tailing and efficiency limitation in kesterite solar cells. Applied Physics Letters. 2013;**103**(10):103506. DOI: 10.1063/1.4820250

[122] Chirilă A, Buecheler S, Pianezzi F, Bloesch P, Gretener C, Uhl AR, et al. Highly efficient Cu(In,Ga)Se2 solar cells grown on flexible polymer films. Nature Materials. 2011;**10**(11):857-861. DOI: 10.1038/nmat3122

[123] Su Z, Tan JMR, Li X, Zeng X, Batabyal SK, Wong LH. Cation substitution of solution-processed Cu2ZnSnS4 thin film solar cell with over 9% efficiency. Advanced Energy Materials. 2015;**5**(19):1500682. DOI: 10.1002/aenm.201500682

[124] Yan C, Sun K, Huang J, Johnston S, Liu F, Veettil BP, et al. Beyond 11% efficient sulfide Kesterite Cu2ZnxCd1–xSnS4 solar cell: Effects of Cadmium alloying. ACS Energy Letters. 2017;**2**(4):930-936. DOI: 10.1021/acsenergylett.7b00129

[125] Hages CJ, Levcenco S, Miskin CK, Alsmeier JH, Abou-Ras D, Wilks RG, et al. Improved performance of Ge-alloyed CZTGeSSe thin-film solar cells through control of elemental losses. Progress in Photovoltaics: Research and Applications. 2015;**23**(3):376-384. DOI: 10.1002/pip.2442

[126] Rey G, Redinger A, Sendler J, Weiss TP, Thevenin M, Guennou M, et al. The band gap of Cu2ZnSnSe4: Effect of order-disorder. Applied Physics Letters. 2014;**105**(11):112106. DOI: 10.1063/1.4896315

[127] Scragg JJS, Choubrac L, Lafond A, Ericson T, Platzer-Björkman C. A low-temperature order-disorder transition in Cu2ZnSnS4 thin films. Applied Physics Letters. 2014;**104**(4):041911. DOI: 10.1063/1.4863685

[128] Gong Y, Zhang Y, Zhu Q, Zhou Y, Qiu R, Niu C, et al. Identifying the origin of the Voc deficit of kesterite solar cells from the two grain growth mechanisms induced by Sn2+ and Sn4+ precursors in DMSO solution. Energy & Environmental Science. 2021;**14**(4):2369-2380. DOI: 10.1039/D0EE03702H

[129] Yang K-J, Kim S, Kim S-Y, Ahn K, Son D-H, Kim S-H, et al. Flexible Cu2ZnSn(S,Se)4 solar cells with over 10% efficiency and methods of enlarging the cell area. Nature

Communications. 2019;**10**(1):2959. DOI: 10.1038/s41467-019-10890-x

[130] Ericson T, Scragg JJ, Hultqvist A, Wätjen JT, Szaniawski P, Törndahl T, et al. Zn(O, S) buffer layers and thickness variations of CdS buffer for Cu2ZnSnS4 solar cells. IEEE Journal of Photovoltaics. 2014;**4**(1):465-469. DOI: 10.1109/JPHOTOV.2013.2283058

[131] Li J, Huang L, Hou J, Wu X, Niu J, Chen G, et al. Effects of substrate orientation and solution movement in chemical bath deposition on Zn(O,S) buffer layer and Cu(In,Ga)Se2 thin film solar cells. Nano Energy. 2019;**58**:427-436. DOI: 10.1016/j.nanoen.2019.01.054

[132] Cui X, Sun K, Huang J, Lee C-Y, Yan C, Sun H, et al. Enhanced heterojunction interface quality to achieve 9.3% efficient Cd-free Cu2ZnSnS4 solar cells using atomic layer deposition ZnSnO buffer layer. Chemistry of Materials. 2018;**30**(21):7860-7871. DOI: 10.1021/acs.chemmater.8b03398

[133] Larsen JK, Larsson F, Törndahl T, Saini N, Riekehr L, Ren Y, et al. Cadmium free Cu2ZnSnS4 solar cells with 9.7% efficiency. Advanced Energy Materials. 2019;**9**(21):1900439. DOI: 10.1002/aenm.201900439

[134] Yuan Z-K, Chen S, Xiang H, Gong X-G, Walsh A, Park J-S, et al. Engineering solar cell absorbers by exploring the band alignment and defect disparity: The case of Cu- and Ag-based Kesterite compounds. Advanced Functional Materials. 2015;**25**(43):6733-6743. DOI: 10.1002/adfm.201502272

[135] Sun H, Sun K, Huang J, Yan C, Liu F, Park J, et al. Efficiency enhancement of Kesterite Cu2ZnSnS4 solar cells via solution-processed ultrathin Tin oxide intermediate layer at absorber/buffer interface. ACS Applied Energy Materials. 2018;**1**(1):154-160. DOI: 10.1021/acsaem.7b00044

[136] Huang TJ, Yin X, Qi G, Gong H. CZTS-based materials and interfaces and their effects on the performance of thin film solar cells. Physica status solidi (RRL) - Rapid Research Letters. 2014;**08**(09):735-762. DOI: 10.1002/pssr.201409219

[137] Tai KF, Gunawan O, Kuwahara M, Chen S, Mhaisalkar SG, Huan CHA, et al. Fill factor losses in Cu2ZnSn(SxSe1−x)4 solar cells: Insights from physical and electrical characterization of devices and exfoliated films. Advanced Energy Materials. 2016;**6**(3):1501609. DOI: 10.1002/aenm.201501609

[138] Scragg JJ, Wätjen JT, Edoff M, Ericson T, Kubart T, Platzer-Björkman C. A detrimental reaction at the molybdenum back contact in Cu2ZnSn(S,Se)4 thin-film solar cells. Journal of the American Chemical Society. 2012;**134**(47):19330-19333. DOI: 10.1021/ja308862n

[139] Scragg JJ, Kubart T, Wätjen JT, Ericson T, Linnarsson MK, Platzer-Björkman C. Effects of back contact instability on Cu2ZnSnS4 devices and processes. Chemistry of Materials. 2013;**25**(15):3162-3171. DOI: 10.1021/cm4015223

[140] Liu F, Sun K, Li W, Yan C, Cui H, Jiang L, et al. Enhancing the Cu2ZnSnS4 solar cell efficiency by back contact modification: Inserting a thin TiB2 intermediate layer at Cu2ZnSnS4/Mo interface. Applied Physics Letters. 2014;**104**(5):051105. DOI: 10.1063/1.4863736

[141] Liu F, Huang J, Sun K, Yan C, Shen Y, Park J, et al. Beyond 8% ultrathin kesterite Cu2ZnSnS4 solar cells by interface reaction route controlling and self-organized nanopattern at the back contact. NPG Asia Materials. 2017;**9**(7):e401. DOI: 10.1038/am.2017.103